Developmental Cell
Article

Prepatterning of Developmental Gene Expression by Modified Histones before Zygotic Genome Activation

Leif C. Lindeman,[1,6] Ingrid S. Andersen,[1,6] Andrew H. Reiner,[1] Nan Li,[2] Håvard Aanes,[3] Olga Østrup,[1,4] Cecilia Winata,[5] Sinnakaruppan Mathavan,[5] Ferenc Müller,[2] Peter Aleström,[3] and Philippe Collas[1,*]
[1]Stem Cell Epigenetics Laboratory, Institute of Basic Medical Sciences, Faculty of Medicine, University of Oslo, and Norwegian Center for Stem Cell Research, 0317 Oslo, Norway
[2]Institute of Biomedical Research, School of Clinical and Experimental Medicine, College of Medical and Dental Sciences, University of Birmingham, B1S 2TT Birmingham, UK
[3]BasAM, Norwegian School of Veterinary Science, 0033 Oslo, Norway
[4]IBHV, LIFE, University of Copenhagen, 1870 Frederiksberg C, Denmark
[5]Stem Cell and Developmental Biology, Genome Institute of Singapore, 138672 Biopolis, Singapore
[6]These authors contributed equally to this work
*Correspondence: philippe.collas@medisin.uio.no
DOI 10.1016/j.devcel.2011.10.008

SUMMARY

A hallmark of anamniote vertebrate development is a window of embryonic transcription-independent cell divisions before onset of zygotic genome activation (ZGA). Chromatin determinants of ZGA are unexplored; however, marking of developmental genes by modified histones in sperm suggests a predictive role of histone marks for ZGA. In zebrafish, pre-ZGA development for ten cell cycles provides an opportunity to examine whether genomic enrichment in modified histones is present before initiation of transcription. By profiling histone H3 trimethylation on all zebrafish promoters before and after ZGA, we demonstrate here an epigenetic prepatterning of developmental gene expression. This involves pre-ZGA marking of transcriptionally inactive genes involved in homeostatic and developmental regulation by permissive H3K4me3 with or without repressive H3K9me3 or H3K27me3. Our data suggest that histone modifications are instructive for the developmental gene expression program.

INTRODUCTION

Gene expression regulation is enabled by the alteration of chromatin states through epigenetic mechanisms involving DNA methylation and posttranslational histone modifications. Histone modifications can modulate DNA-histone interactions and serve to recruit proteins by recognition of the modified histones through specific domains; these factors, in turn, remodel chromatin to promote or repress transcription (Ruthenburg et al., 2007). Among histone modifications the most extensively characterized, trimethylation of lysine 4 of histone H3 (H3K4me3) marks the transcription start site (TSS) of active genes, as well as in the absence of transcription, while promoter occupancy by H3K27me3 or H3K9me3 promotes transcriptional repression. In contrast, H3K36me3 is commonly found on gene bodies in association with transcription elongation (Kolasinska-Zwierz et al., 2009). Histone modifications are thus associated with gene regulation events.

Histone modifications may also serve a predictive function for gene expression. In embryonic stem (ES) cells, coenrichment in H3K4me3 and H3K27me3 encompasses chromatin domains containing developmentally regulated genes poised for transcriptional activation (Azuara et al., 2006; Bernstein et al., 2006). H3K4me3/K27me3 coenrichment has been identified in somatic progenitors (Cui et al., 2009), differentiated cells (Barski et al., 2007; Lindeman et al., 2010a), and zebrafish embryos (Vastenhouw et al., 2010) and may constitute a mark predictive of gene expression potential. However, coenrichment is not predominant in embryos of *Xenopus* (Akkers et al., 2009) or *Drosophila* (Schuettengruber et al., 2009). Combinatorial coincidence of other histone modifications may convey additional predictive functions (Wang et al., 2008; Kharchenko et al., 2011; Ernst et al., 2011).

Relevant to the idea of a prepatterning of gene expression by histone modifications are findings that mouse and human sperm contain histones (in addition to protamines), some of which are marked by H3K4me2/3 and H3K27me3 (Hammoud et al., 2009; Brykczynska et al., 2010). Zebrafish sperm, which lack protamines, also harbor H3K4me3, H3K27me3, H3K9me3, and H3K36me3 (Wu et al., 2011). Gene ontology (GO) highlights homeostatic and developmental functions for H3K4me3-marked genes and developmental functions for genes marked by H3K27me3 (Wu et al., 2011). Moreover, sperm from pig (Jeong et al., 2007) and *Xenopus* (Shechter et al., 2009) contain H3K9me3. These observations lead to the suggestion of transmission of permissive and repressive instructions from gamete to embryo through fertilization (Puschendorf et al., 2008; Brykczynska et al., 2010; Arico et al., 2011; Wu et al., 2011).

An inheritance model implies detection of modified histones during early development. While immunostaining of mouse pronuclei and blastomeres supports this view (Albert and Peters, 2009; Puschendorf et al., 2008), chromatin immunoprecipitation

(ChIP) data in *Xenopus* and zebrafish embryos show genomic enrichment in H3K4me3 or H3K27me3 from the time of zygotic gene activation (ZGA) onward (Akkers et al., 2009; Lindeman et al., 2010b; Vastenhouw et al., 2010; Aday et al., 2011). These observations imply that histone modifications may confer regulatory functions at the time of ZGA; however, they leave the question open of whether an epigenetic prepatterning exists prior to ZGA.

In zebrafish, ZGA onset occurs at the mid-blastula transition (MBT) 3.3 hr postfertilization (hpf) and is associated with lengthening of the cell cycle and increase in the nuclear/cytoplasmic ratio (Tadros and Lipshitz, 2009). Prior to the MBT, embryonic genes are silent (Kane and Kimmel, 1993) and our recent RNA-sequencing (RNA-seq) profiling of the early zebrafish transcriptome (Aanes et al., 2011) questions evidence of pre-MBT transcription (Leung et al., 2003; Mathavan et al., 2005). Pre-MBT development proceeds from maternal pools of mRNAs and has been shown to occur in the absence of transcription (Müller et al., 2001).

Zebrafish pre-MBT stages last for ten cell cycles and provide an ideal opportunity to test the hypothesis of pre-ZGA epigenetic patterning of the developmental program in the absence of transcription. By profiling histone methylation on promoters before and at the time of ZGA, we demonstrate here the marking of homeostatic and developmentally regulated genes by permissive and repressive histone marks before ZGA onset. Our data are consistent with a pre-ZGA patterning of the embryonic transcriptional program by modified histones and suggest an instructive role of epigenetic modifications in developmental gene expression.

RESULTS

Establishment of Chromatin States during Early Development

To address how embryos are epigenetically programmed prior to ZGA, we profiled by ChIP-chip the occupancy of promoters and 5′ end of genes by H3K4me3, a permissive modification, H3K27me3, a mark associated with inactive promoters, H3K36me3, a mark of transcription elongation found on gene bodies, and H3K9me3, another modification associated with inactive promoters. We also interrogated RNA polymerase II (RNAPII) occupancy using an antibody against the NH_2-terminal domain, recognizing unphosphorylated and phosphorylated forms of RNAPII, to assess transcriptional poising and elongation. To this end, we used a sensitive ChIP assay that we optimized for early stage zebrafish embryos (Lindeman et al., 2009). Embryos were analyzed before ZGA at the 256-cell stage (2.5 hpf, "pre-MBT"; this time point enables recovery of chromatin in sufficient amounts for ChIP); during ZGA onset (3.3 hpf, "MBT") and after ZGA onset (50% epiboly; 5.3 hpf, "post-MBT"; Figure 1A). Data were analyzed in the context of our recent RNA-seq analysis of unfertilized eggs, 1-cell, 16-cell, 128/256-cell (pre-MBT), MBT, and post-MBT embryos (Aanes et al., 2011). ChIP DNA was hybridized to a high-density microarray tiling 15 kb of upstream regulatory sequence and 5 kb downstream of the TSS of all zebrafish genes including 12,697 RefSeq genes (Lindeman et al., 2010a) (Figure 1A). Peaks of enrichment were detected using MA2C with $p \leq 10^{-4}$ and enriched regions were assigned to RefSeq genes. ChIP-chip data were normalized to input chromatin used in each ChIP, determined by A_{260}, which was kept constant for each stage examined. This eliminated potential bias that might have been caused by inefficient chromatin preparation from small cell numbers.

This approach reveals developmental stage-dependent enrichment in trimethylated H3K4, H3K27, H3K9, H3K36, and in RNAPII (Figures 1B and 1C; see Figure S1 available online; see Table S1 for gene lists). We detect H3K4me3 enrichment on over 1000 genes as early as the 256-cell stage (pre-MBT) and on over 9000 genes at MBT and post-MBT stages (Figure 1C). On a subset of genes, the level of H3K4me3 increases between pre-MBT and MBT as genes become transcriptionally competent (Figure 1B). This is observed for maternally expressed genes, which are not transcribed per se pre-MBT but become upregulated after the MBT (Figures 1B and 1D; *bactin1*, *pou5f1*; Table S2) (Aanes et al., 2011), and for zygotic genes which are not expressed until after the MBT (*akap12*, *tbx16*). H3K4me3 enrichment peaks at the TSS (Figure 1B; *dachb, uba3*), or occurs as larger blocks including the coding region (Figure 1B, *bactin1, pou5f1, akap12, tbx16*) or entire loci such as *hox* loci (Figure 1B; *hoxb1b*; Figure S2A). H3K27me3 and H3K9me3 are also detected pre-MBT yet on fewer genes than H3K4me3 (Figure 1C), with H3K27me3 also peaking at the TSS (Figure 1B; *dachb*) or covering genes (Figure 1B, *hoxb1b*; Figure S2A). Subsequently, H3K27me3 globally precedes H3K9me3, which occurs between MBT and post-MBT stages (Figure 1C). H3K36me3 is detected from the MBT onward together with variable levels of RNAPII, primarily on the coding region of genes upregulated after the MBT (Figures 1B–1D). This is particularly evident on genes expressed maternally (i.e., with transcripts detected pre-MBT) and upregulated after MBT (Figure 1B, *bactin1*, *pou5f1*) as well as on zygotic genes (Figures 1B and 1D; *akap12*, *tbx16*). Altogether, these results reveal stage-dependent genomic enrichment in H3K4, K9, K27 and K36 trimethylation. H3K4me3, H3K9me3 and H3K27me3 are detected as early as the 256-cell stage, suggesting mechanisms of transcriptional repression already in place at this stage.

Low abundance of modified histones and low nuclear/cytoplasmic ratios at the pre-MBT stage pose a technical challenge for ChIP. Thus, we validated our results by several independent approaches. We first show H3K4me3, H3K27me3 and H3K9me3 occupancy by quantitative (q)PCR tiling of single genes after triplicate ChIPs for each modification (Figures 2A and 2B). These genes were randomly selected among those enriched in H3K4me3 pre-MBT irrespective of H3K27 or H3K9me3 enrichment or localization within the tiled region (see also Figure 2A). These data are substantiated by three additional ChIP-qPCRs using different anti-H3K4me3 and H3K27me3 antibodies (Figure S2B). Moreover, as our ChIP protocol involves a DNA-protein crosslinking step, we confirm by native carrier ChIP, which does not involve crosslinking (O'Neill et al., 2006), H3K4me3, H3K9me3, and H3K27me3 occupancy at the pre-MBT stage (Figure 2C). Western blotting confirms the presence of H3K4me3 as early as the 256-cell stage (Figure 2D). Lastly, we show H3K4me3 by immunofluorescence using two different antibodies in interphase nuclei of 128-cell, 256-cell, 512-cell, and dome stage embryos (Figure 2E, arrows; Figure S2C). Of

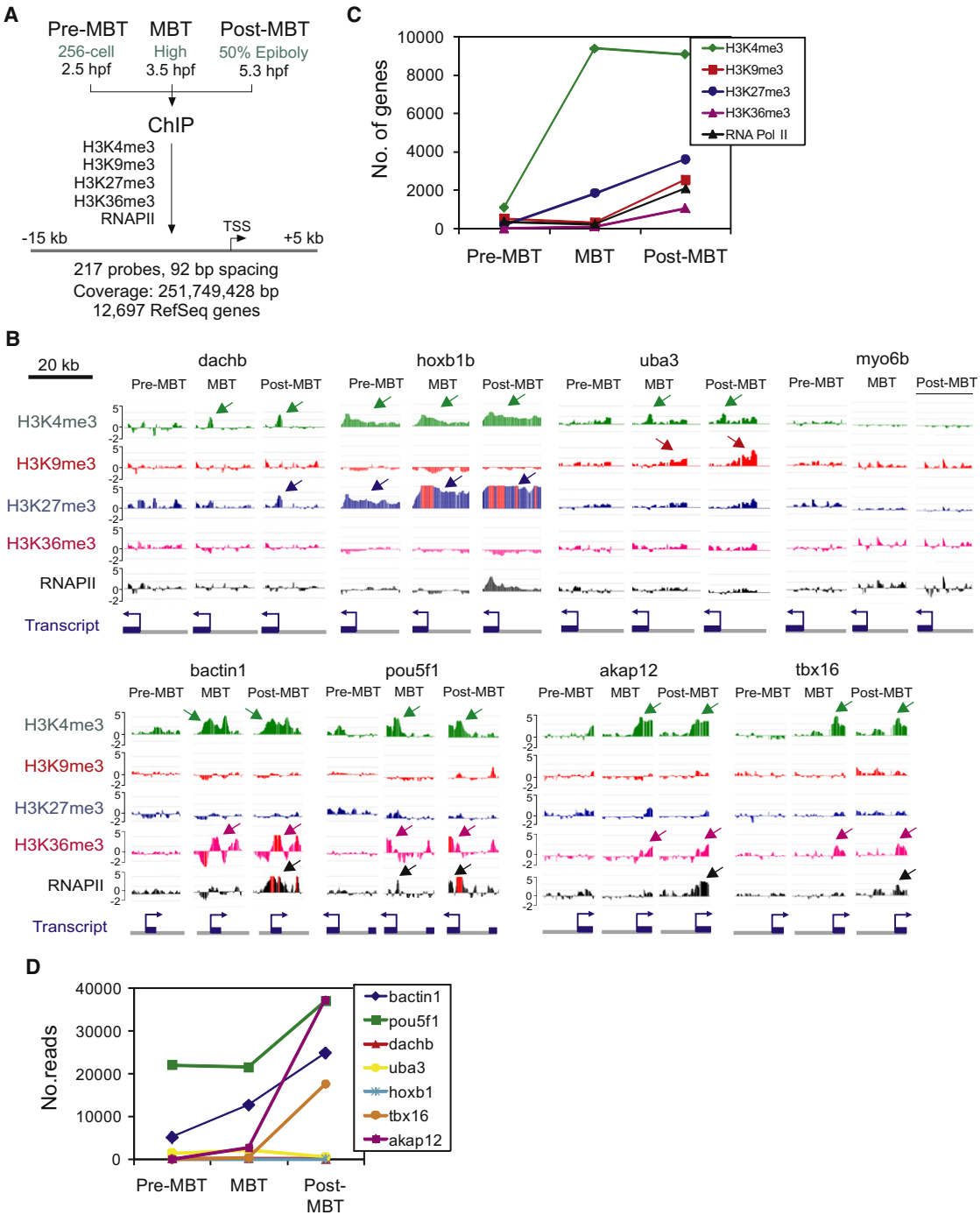

Figure 1. Developmental Stage-Specific Enrichment in Trimethylated H3K4, H3K9, H3K27, H3K36, and RNAPII

(A) Experimental design.

(B) ChIP-chip profiles of histone H3 methylation and RNAPII occupancy on indicated genes (MA2C scores) at pre-MBT, MBT, and post-MBT stages. Arrows point to enriched areas. Red bars indicate out-of-scale scores. *myo6b* is shown as a gene not enriched at the stages examined.

(C) Developmental enrichment in H3K4me3, H3K9me3, H3K27me3, H3K36me3, and RNAPII.

(D) RNA-seq expression profile of genes shown in (B).

note, H3K4me3 is also detected on mitotic chromosomes at each stage (Figure 2E, arrowheads). This is in line with identification of H3K4me3 domains on metaphase chromosomes of somatic cells (Terrenoire et al., 2010) and suggests continuity of histone modification marks during the synchronous cell cycles of pre-MBT stage embryos. These results demonstrate H3K4me3, H3K9me3 and H3K27me3 enrichment on a subset of genes as early as the 256-cell stage, consistent with a

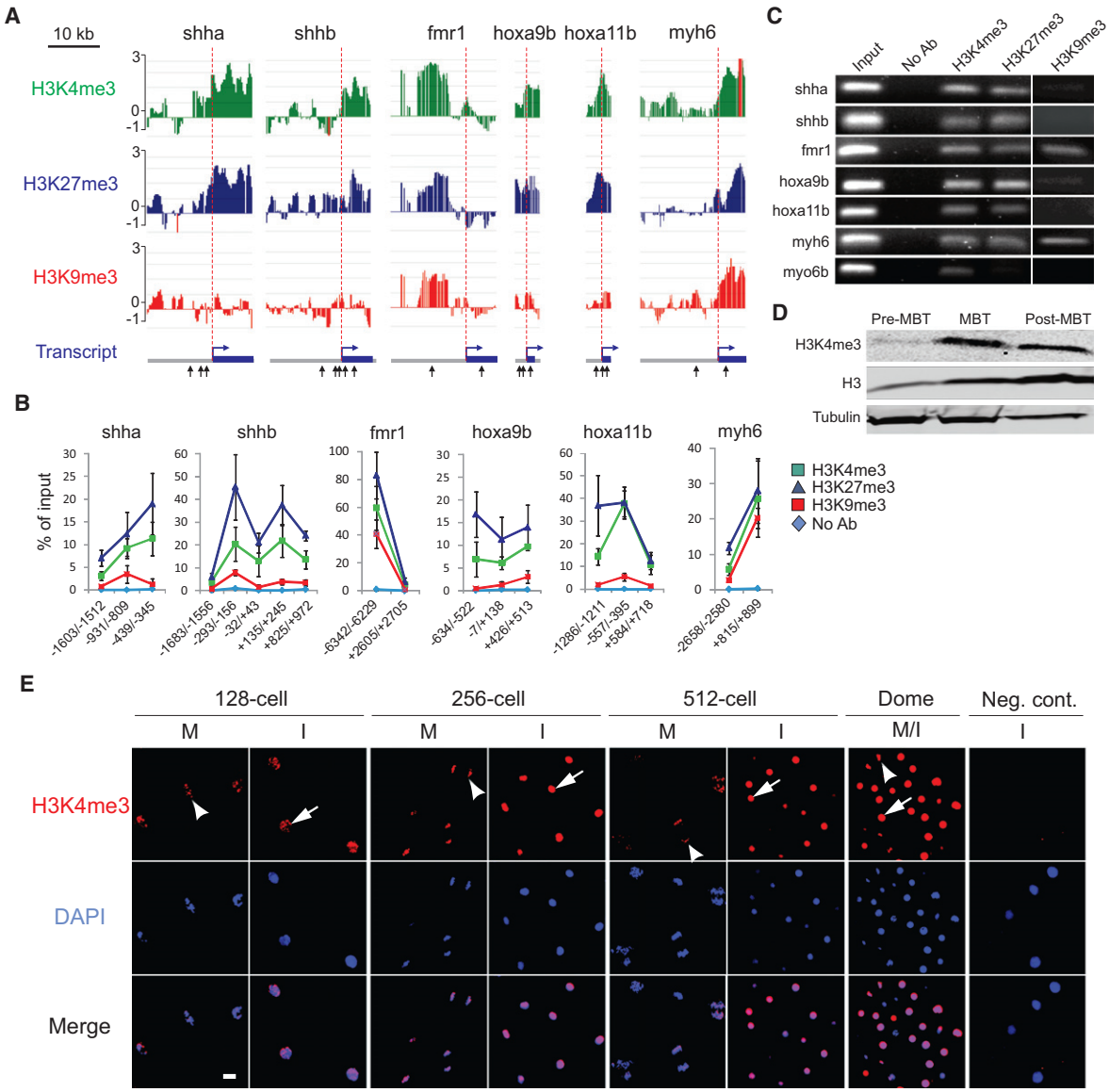

Figure 2. Enrichment in H3K4me3, H3K27me3, and H3K9me3 at the Pre-MBT Stage

(A) H3K4me3, H3K27me3, and H3K9me3 ChIP-chip profiles on indicated genes at the pre-MBT stage (MA2C scores). Genes were ranked as follows, in decreasing order, among the 1081 genes enriched in H3K4me3 pre-MBT: *shha* (107), *fmr1* (226), *hoxa9b* (284), *hoxa11b* (464), *myh6* (679); *shhb* was also selected for its H3K4me3 marking (though not enrichment) in the absence of H3K9me3. Arrows (bottom track) mark amplicons examined by ChIP-qPCR in (B).

(B) ChIP-qPCR validation of H3K4me3, H3K27me3, and H3K9me3 pre-MBT marking on indicated genes (mean ± SD of three ChIPs with each antibody).

(C) Native ChIP-PCR validation of H3K4me3, H3K27me3, and H3K9me3 occupancy.

(D) Western blot analysis of H3K4me3 in developing embryos.

(E) Immunofluorescence detection of H3K4me3 in the animal pole of embryos at indicated stages. Arrows and arrowheads point to labeled nuclei and metaphases, respectively. Signal intensity is adjusted to 128-cell images. Time points: 128-cell, 2.2 hpf; 256-cell, 2.5 hpf; 512-cell, 2.7 hpf; Dome, 4.3 hpf. I, interphase; M, metaphase. Scale bar, 10 μm.

pre-ZGA marking of the genome by posttranslationally modified histones.

H3K4me3-Marked Genes at the 256-Cell Stage Are Transcriptionally Inactive

Pre-ZGA genome marking by H3K4me3 implies that genes occupied by H3K4me3 at the 256-cell stage are not transcribed at this stage. Prior to the MBT, embryonic genes are inactive (Kane and Kimmel, 1993). To ascertain that H3K4me3-marked genes are not transcribed pre-MBT, we first show that these genes have no H3K36me3 and no exon-bound RNAPII (Figure 3A; when detected, RNAPII is on the promoter; Figure 3B). Next, we assessed the presence of transcripts pre-MBT using our RNA-seq data. We classified transcripts as "detected" and

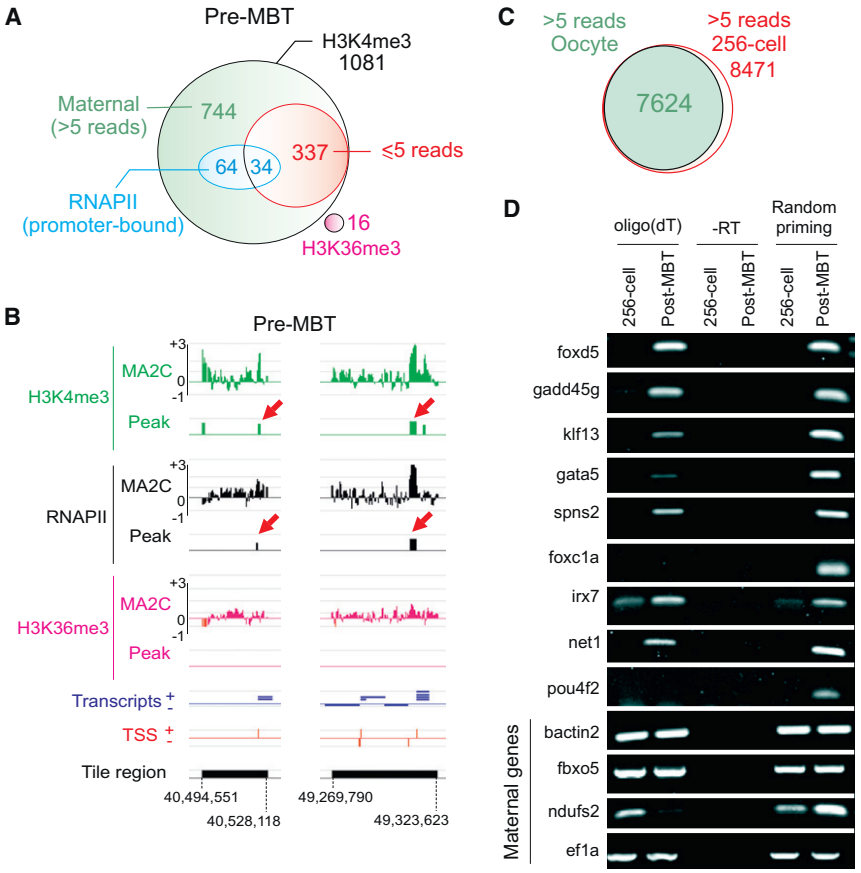

Figure 3. H3K4me3 Marks Transcriptionally Inactive Genes Prior to ZGA

(A) Venn diagram analysis of pre-MBT H3K4me3-marked genes in relation to RNAPII, H3K36me3, and transcript detection by RNA-seq.

(B) Pre-MBT RNAPII enrichment on H3K4me3-marked genes coincides with promoters. MA2C and peak scores are shown. Arrows point to TSS enrichment. Tiled regions are delineated by nucleotide number (chromosome 1; left: NM_001080190; right, in the 5′→3′ orientation: *spark*, *zgc:92638*, *presenilin2*, *zgc:112208*).

(C) Overlap between genes with detected transcripts at the pre-MBT (256-cell) stage and in oocytes.

(D) RT-PCR analysis of expression of indicated H3K4me3-marked genes at the pre-MBT (256-cell) and post-MBT stages, using oligo(dT) or random priming for cDNA synthesis. Transcripts from known maternal genes were used as positive controls. PCR without RT (-RT) was done as negative control.

"nondetected" if greater than five reads or five or fewer reads, respectively, were mapped to them (see Experimental Procedures). We find that 31% (n = 337) of the pre-MBT H3K4me3-marked genes have no transcript at this stage (Figure 3A). Genes with a corresponding transcript are maternally expressed because they lack coding region-bound RNAPII or H3K36me3 (Figure 3A) and they are also found in unfertilized eggs (Figure 3C). Further, since RNA-seq data were generated from poly(A)$^+$ mRNA, some of the H3K4me3-marked genes may be transcribed but the RNA is not polyadenylated. Thus, we confirm the lack of transcription of a subset of the pre-MBT H3K4me3-marked genes, by RT-PCR using as template cDNA synthesized from oligo(dT) beads or by random priming (Figure 3D). We conclude that pre-MBT H3K4me3-marked genes are not transcribed, and that H3K4me3 enrichment at this stage is not indicative of transcriptional activity.

Multivalent and Dynamic Chromatin Signatures during Early Development

Stage-specific enrichment in H3K4me3, H3K9me3, and H3K27me3 in embryos prompts the determination of whether pre-MBT H3K4me3-marked genes acquire a repressive mark later in development. To this end, we established an epigenetic fate map of the pre-MBT H3K4me3-marked genes (Figure 4A; Figures S3A and S3B). Remarkably, 18% of these genes are already coenriched in H3K27me3 and/or H3K9me3 at the pre-MBT stage (Figure 4A). Among "H3K4me3-only" genes, we find that the majority gain H3K27me3 or less frequently H3K9me3 at the MBT or post-MBT stages (Figures 4A and 4B), and the vast majority of these genes retain the acquired repressive mark(s) post-MBT (Figure 4A; Figure S3B).

Next, coenrichment of H3K4me3 with repressive marks prompted the evaluation of the coincidence of these marks within the tiled regions. We detect promoters enriched in H3K4me3 together with H3K27me3, H3K9me3, or both marks (Figures 4A and 4C; Figure S3C). The numbers of coenriched promoters increases dramatically from pre-MBT to post-MBT, with H3K4me3/K27me3 prevailing at the MBT whereas H3K4me3/K9me3 and H3K4me3/K9me3/K27me3 coincidence substantially increases post-MBT (Figure 4C). H3K4me3/K9me3/K27me3 coenrichment is reminiscent of recent findings in mammalian ES cells (Bilodeau et al., 2009; Hawkins et al., 2010) suggesting that despite the species difference, ES cells may retain this embryonic feature.

Trimethylation of H3K4, K9, and K27 Marks Functionally Distinct Gene Sets before ZGA

To evaluate the significance of pre-MBT enrichment in trimethylated H3K4, H3K9, or H3K27, we determined GO terms enriched for the corresponding genes at this stage (Figure 4D; Table S3). H3K4me3 genes are most significantly involved in cellular homeostasis including metabolic and synthetic processes, as well as in transcription regulation and embryonic development (including members of the *bhlh*, *cebp*, *fox*, *gata*, *hox*, *nkx*, *pou*, *runx*, *sox* and *tbx* gene families). Differential repressive histone marking delineates already at the pre-MBT stage distinct functional categories: H3K27me3-marked genes are associated with transcription regulation and development (Figure 4D), and while no enriched GO terms are found for H3K9me3, examination of all GO terms reveals cell adhesion/migration, cell cycle and transport (data not shown). Among the pre-MBT H3K4me3-marked genes

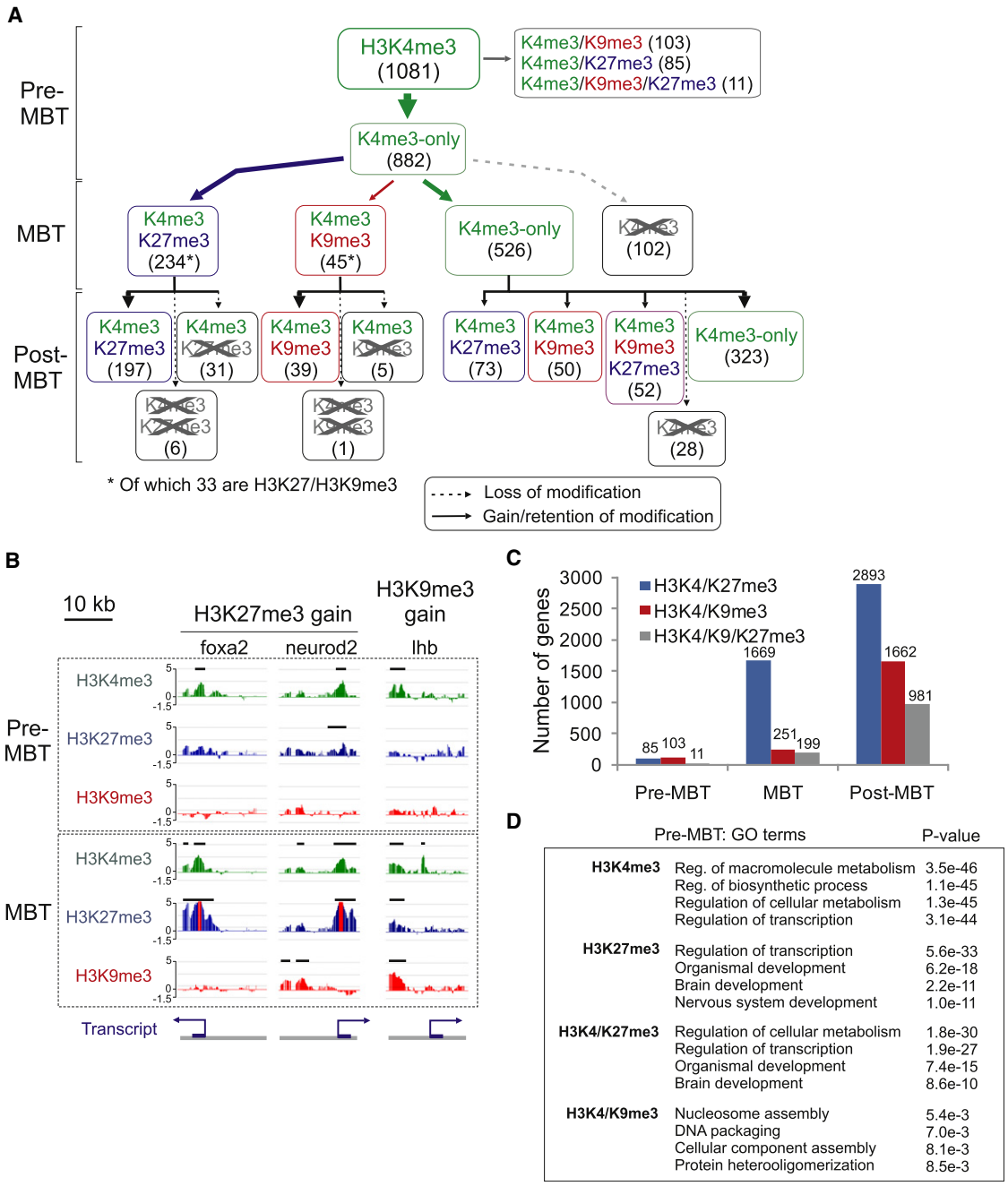

Figure 4. Epigenetic Fate of Genes Marked by H3K4me3 Pre-MBT

(A) Epigenetic fate map of pre-MBT H3K4me3-marked genes (supporting Venn diagrams are shown in Figure S3A). Epigenetic signatures are shown with corresponding numbers of genes. Arrow thickness reflects the numbers of genes concerned by a given change.

(B) Examples of pre-MBT H3K4me3-marked genes that gain H3K27me3 or H3K9me3 at the MBT stage (MA2C scores). Horizontal bars visualize significant enrichment peaks ($p < 10^{-4}$).

(C) Coenrichment in H3H4me3, H3K9me3 and H3K27me3 during development.

(D) Most significant GO terms associated with indicated histone modifications at the pre-MBT stage.

coenriched in H3K27me3 or H3K9me3, H3K27me3 targets genes involved in metabolism, transcription regulation and development, while H3K9me3 targets genes involved in chromatin assembly (Figure 4D). The developmental functions linked to H3K4me3/K27me3-enriched genes are consistent with those associated with H3K4me3/K27me3 "bivalency" in ES cells (Bernstein et al., 2006; Pan et al., 2007) and mouse embryos (Dahl et al., 2010). Our data indicate therefore that an early step of the developmental program entails the marking of promoters with important homeostatic and developmental functions prior to ZGA onset.

After ZGA onset, H3K4me3/K27me3 remains mainly associated with developmental functions, as well as cell projection and migration processes (Table S3); the latter is particularly relevant in the context of cell movements characterizing gastrulation, which starts post-MBT. H3K4me3/K9me3-marked genes are in contrast enriched in G protein signaling functions (Table S3). We also note a broadening of GO terms enriched among H3K4me3-marked genes post-MBT, consistent with somatic cell data (Barski et al., 2007; Lindeman et al., 2010b).

Pre-MBT H3K4me3 Marking Suggests a Predictive Role for the Embryonic Transcription Program

Premarking of homeostasis and developmental genes by H3K4me3 before ZGA is suggestive of a developmental instructive function of pre-MBT H3K4me3 marking. One would then expect that a significant fraction of these genes are expressed at or after ZGA, and that these genes would functionally cluster differently from expressed genes that are not marked by H3K4me3 pre-MBT. Indeed, using our RNaseq data, we first find that pre-MBT H3K4me3 genes are enriched among those expressed from the MBT onward relative to the proportion of all upregulated RefSeq genes ($p < 10^{-5}$, Figure 5A). This is in line with the number of pre-MBT H3K4me3 genes enriched in RNAPII at the post-MBT stage (Figure S4C). The homeostatic and developmental functions of the pre-MBT H3K4me3-marked genes are also in line with their transcriptional induction after ZGA. Further, most genes not expressed or enriched in RNAPII post-MBT are held in a repressive mode by H3K9me3 and/or H3K27me3 pre-MBT (data not shown). Second, pre-MBT H4K3me3-marked genes are more strongly expressed than all RefSeq genes at the MBT stage ($p = 2 \times 10^{-16}$, Wilcoxon rank sum test; Figure 5B). Thus, pre-MBT H3K4me3 enrichment is strongly associated with a propensity for transcriptional activation after ZGA; this is consistent with a predictive function of pre-MBT H3K4me3 marking for the embryonic gene expression program.

Third, among genes that become expressed after ZGA, pre-MBT H3K4me3 marking defines a subset of genes with distinct GO terms relative to expressed genes not marked by H3K4me3 pre-MBT: H3K4me3-marked genes are most significantly associated with transcription regulation functions (Figure 5C) while unmarked genes directly pertain to development (Figure 5D). Therefore, not only does H3K4me3 target developmentally regulated genes at the pre-MBT stage, it also clusters genes with specific developmental functions.

Overlap between H4K3me3-Marked Genes in Sperm and in Pre-MBT Stage Embryos

Recent epigenetic profiling of zebrafish sperm indicates that genes needed for embryonic development are marked by combinations of histone modifications including H3K4me3 and H3K27me3 (Wu et al., 2011). This observation enables a closer look at the hypothesis of transgenerational inheritance of histone marks. Comparing the top 800 genes enriched in H3K4me3 or H3K27me3 in sperm with pre-MBT-marked genes, we find 97 and 81, respectively, overlapping genes, making up 9% and 40% of the pre-MBT H3K4me3- and H3K27me3-marked genes (Figure 6A). Remarkably, 94% of the genes marked by H3K4me3 in both sperm and embryos are expressed at MBT or post-MBT

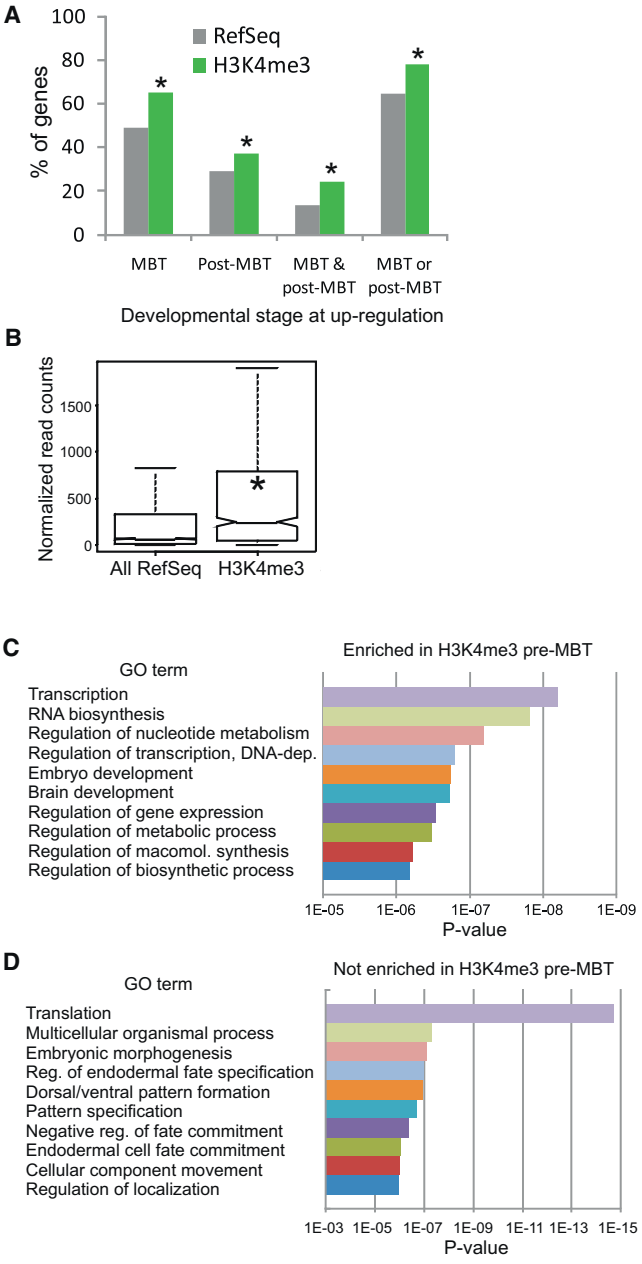

Figure 5. Pre-MBT H3K4me3-Marked Genes Are Preferentially Expressed Later in Development

(A) Percentage of genes expressed at indicated stages (x axis) that are enriched in H3K4me3 pre-MBT (green bars) versus all expressed RefSeq genes (gray bars). *$p < 10^{-5}$ relative to all.

(B) Box plot analysis of gene expression levels at the MBT stage (RNA-seq), for pre-MBT H3K4me3-marked genes versus all RefSeq genes. *$p = 2 \times 10^{-16}$ relative to all.

(C and D) Top 10 enriched GO terms among genes expressed at the MBT stage, and that are either (C) enriched or (D) not enriched in H3K4me3 pre-MBT.

(Figure 6C), which is far above the proportion of all RefSeq genes becoming expressed at these stages (see Figure 5A; $p < 10^{-5}$). This proportion is strikingly identical to that of H3K4me3-marked genes in "sperm only" that become expressed, and greater than

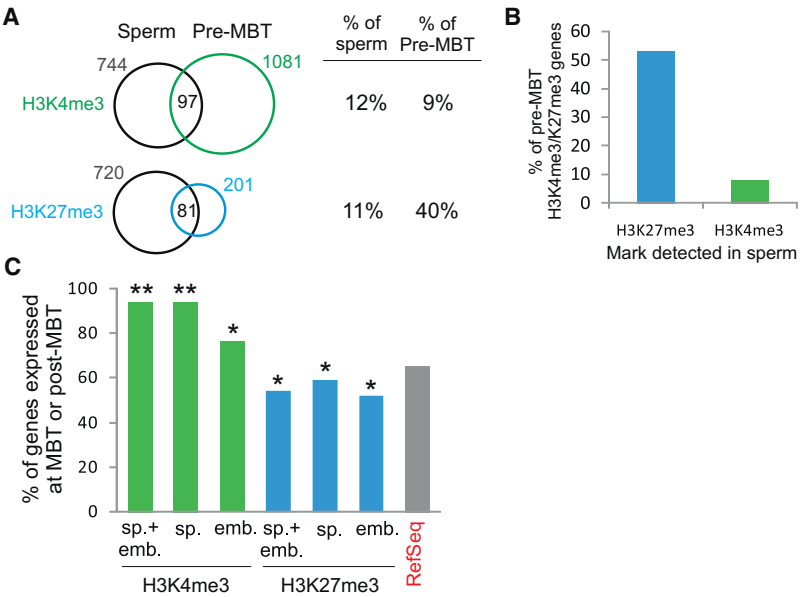

Figure 6. Overlap of Genes Enriched in H3K4me3 or H3K27me3 in Sperm and in Pre-MBT Embryos

(A) Venn diagram analysis of overlapping H3K4me3- or H3K27me3-marked genes in sperm and in pre-MBT embryos, with percentages.

(B) Percentage of pre-MBT H3K4me3/K27me3-enriched genes that are marked by H3K27me3 or H3K4me3 in sperm. Sperm data are from Wu et al. (2011).

(C) Percentage of genes enriched in H3K4me3 or H3K27me3 in sperm (sp.), pre-MBT embryos (emb.) or both, that are expressed or upregulated at the MBT or post-MBT stages.

the fraction of H3K4me3-marked genes at pre-MBT only (Figure 6C). Altogether, this indicates a strong propensity of H3K4me3 to mark genes in sperm that will be expressed at the time of ZGA. The proportion of sperm-only or sperm- and embryo-H3K27me3-marked genes becoming expressed is in contrast lower than that of RefSeq genes (Figure 6C; $p < 10^{-4}$). H3K4me3-marked genes in the sperm and pre-MBT embryo intersect (Figure 6A) are primarily implicated in metabolic processes, whereas H3K27me3 is associated with transcription regulation and developmental functions; these notably include the homeobox gene families *fox*, *hox*, *gbx*, *pax*, *phox*, *six*, *sox*, and *tbx* (Table S4). One should also note that H3K4me2/3 and H3K27me3 genes identified in human and mouse sperm are also respectively enriched in homeostatic and developmental functions (Hammoud et al., 2009; Brykczynska et al., 2010), as in zebrafish embryos. Collectively, these findings are consistent with the suggestion of inheritance of histone modifications from sperm to embryos (Puschendorf et al., 2008; Hammoud et al., 2009; Brykczynska et al., 2010; Wu et al., 2011; Arico et al., 2011), and with an instructive role of histone modifications for the developmental program. Interestingly, we find that 53% of pre-MBT H3K4me3/K27me3 genes are marked by H3K27me3 (without H3K4me3) in sperm, as opposed to 8% that are marked by H3K4me3 (Figure 6B). Our data therefore also raise the hypothesis that the marking of developmentally important genes (such as homeobox genes) by H3K27me3 in sperm may play a role in the establishment of a poised chromatin state in the embryo prior to ZGA.

Histone Methylation Profiles of Developmentally Upregulated Genes

A hallmark of development is a dynamic gene expression profile resulting from up- and downregulation of cohorts of developmentally regulated genes (Aanes et al., 2011; Graveley et al., 2011). It remains unknown, however, whether genes in these clusters are differentially "primed" by specific chromatin states for activation. To address this issue, we defined clusters of genes with distinct mRNA expression profiles and examined the histone methylation profile of these clusters at the pre-MBT, MBT and post-MBT stages (see Experimental Procedures) (Figure 7A). We defined a "maternal-zygotic cluster" consisting of genes with mRNAs detected in unfertilized eggs and significantly upregulated at the MBT or post-MBT stages (608 genes); a "zygotic cluster" consisting of mRNAs detected from the MBT or post-MBT onward (438 genes); and a cluster of genes with no detected transcripts at any stage ("nondetected cluster"; 2990 genes).

Consistent with the lack of transcription pre-MBT, we find that virtually no genes in the zygotic and maternal-zygotic clusters harbor H3K36me3 or RNAPII until after the MBT (Figures 7B and 7C, *spry1*, *bactin2*), when genes become expressed (Figure 7D). As expected, the majority of genes with nondetected transcripts display neither H3K36me3 nor RNAPII (Figure 7B and 7C, *bmpr2a*). A small number of genes not expressed post-MBT (verified by RT-PCR; Figure S4A) nevertheless display H3K36me3 occasionally on the coding region in the absence of RNAPII enrichment (Figure 7C), or on the promoter region (Figure S4B). Promoter enrichment in H3K36me3 has also notably been reported in sperm (Wu et al., 2011) and is consistent with the repressive role of this modification on transcription initiation (Carrozza et al., 2005).

Enrichment in H3K4, K9, and K27 trimethylation is both cluster and stage specific. Throughout developmental stages, genes without detected transcripts contain the highest proportions of "no enrichment" in any of the marks, the lowest proportions of H3K4me3-marked genes, and the highest proportions of repressively marked genes (Figure 7E). Furthermore, ~15% of genes in the zygotic and maternal-zygotic clusters, i.e., upregulated at the MBT or post-MBT, are enriched in H3K4me3 at the pre-MBT stage (Figure 7E). However, at the MBT and post-MBT stages, a greater proportion of maternal-zygotic genes are enriched in H3K4me3 than zygotic genes, suggesting that maternal genes are preferentially targeted for H3K4me3 at the time of ZGA. We also note in the zygotic and maternal-zygotic clusters significant proportions of genes apparently coenriched in H3K4me3 with H3K27me3 and/or H3K9me3 (Figure 7E). As these genes are transcribed, this may reflect a spatial regulation of expression in the embryo (Akkers et al., 2009; Schuettengruber et al., 2009). Collectively, these results indicate that embryonic gene

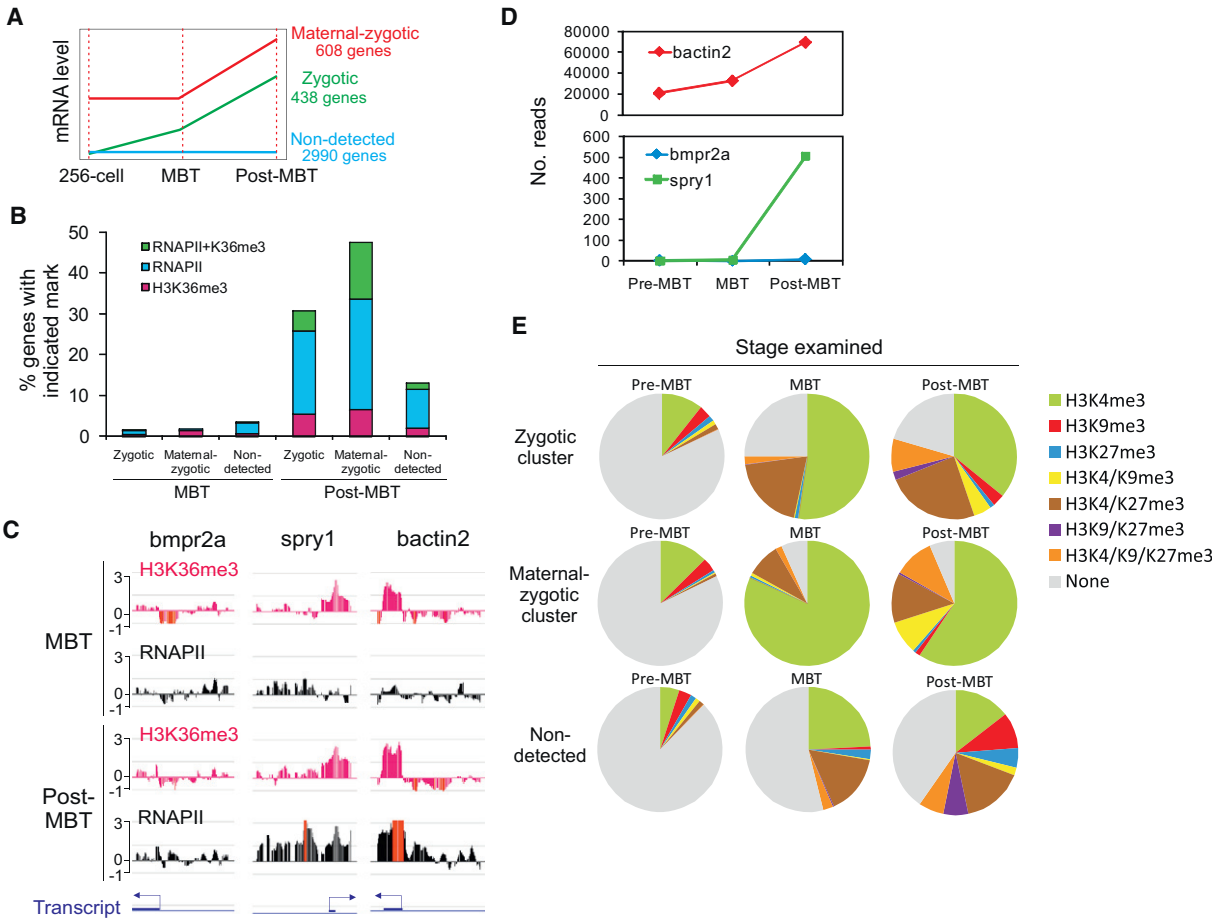

Figure 7. Chromatin States of Developmentally Regulated Gene Clusters

(A) Schematic mRNA expression profiles and numbers of genes in the maternal-zygotic cluster, the zygotic cluster, and genes with nondetected transcripts.

(B) Percentage of genes of each cluster enriched in RNAPII and/or H3K36me3 at MBT and post-MBT stages.

(C) MBT and post-MBT H3K36me3 and RNAPII profiles on a nonexpressed gene (*bmpr2a*), a maternal-zygotic gene (*bactin2*) and a zygotic gene (*spry1*). Note RNAPII enrichment on *spry1* and *bactin2* post-MBT coinciding with transcriptional upregulation (see D).

(D) RNA-seq profile of *bactin2*, *bmpr2a*, and *spyr1*. Values are from Aanes et al. (2011).

(E) Proportions of genes of the zygotic, maternal-zygotic and the nondetected clusters marked by H3K4me3, H3K9me3, H3K27me3 or combinations thereof at the pre-MBT, MBT, and post-MBT stages.

upregulation from the MBT onward correlates with the establishment of complex patterns of promoter enrichment in histone modification. Nonetheless, a significant proportion of genes activated at of after ZGA are marked by modified histones prior to ZGA.

DISCUSSION

We provide evidence of temporal enrichment of promoters in histone H3 methylation marks starting prior to the onset of ZGA during zebrafish development. Our findings demonstrate a pre-ZGA patterning of the developmental transcription program by trimethylation of H3K4, K9, and K27 at the 256-cell stage on genes important for homeostasis, transcription regulation, and development. Consistent with this observation is the detection of transcripts for SET-domain proteins at pre-MBT stages (Sun et al., 2008) and indications by RNA-seq (Aanes et al., 2011) that zebrafish eggs are already loaded with polyadenylated mRNAs for histone methyltransferases of H3K4 (*setdb1a*, *setdb1b*, *mll*, *setd7*), H3K9 (*ehmt2*, *ehmt1a*, *suv39h1b*), and H3K27 (*ezh2*). Pre-MBT genome marking by modified histones is not restricted to trimethylated H3K4, K27 or K9, as histone H4 is also acetylated pre-MBT (Toyama et al., 2008). Interestingly, H4 acetylation mediates preferential binding of the BRD4 transcription factor in vitro (Dey et al., 2003; Toyama et al., 2008), suggesting that acetylated H4 may premark genes for BRD4 targeting and transcription after ZGA onset (Toyama et al., 2008). It should be mentioned that a component of the temporal dynamics of modified histone (or transcription factor) enrichment detected during development may be reduced to detection sensitivity; thus appearance of a mark may not only reflect de novo marking but also a spreading of a preexisting mark, in terms of the number of cells harboring the mark and the number of histone molecules bearing the mark at a given genomic site.

Prepatterning of embryonic gene expression by histone marks is consistent with a model of epigenetic modifications having an

instructive role for the developmental program. An instructive role implies that pre-MBT H3K4me3-marked genes are transcriptionally inactive, as we show here, consistent with the overall transcriptional quiescence at pre-MBT stages (Schier, 2007; Tadros and Lipshitz, 2009). Promoters can be targeted for H3K4 trimethylation in the absence of transcription (Bernstein et al., 2006; Blythe et al., 2010) and genomic context plays a role in this process. Indeed, CpG islands that lack DNA methylation are sufficient for SETD1-mediated H3K4 trimethylation (Thomson et al., 2010). H3K4 trimethylation on target promoters at pre-MBT stages in *Xenopus* embryos may also indirectly involve WNT signaling via β-catenin in a manner temporarily uncoupled from target gene transcription (Blythe et al., 2010). Zebrafish embryos may utilize similar mechanisms for addressing H3K4 trimethylation to promoters prior to ZGA, an issue that remains to be examined.

Early developmental instructions may thus be encoded by enrichment in specific histone marks. Pre-MBT H3K4me3-marked genes are more likely to be activated than unmarked genes, and second, coenrichment in H3K27me3 or H3K9me3 after MBT segregates genes into distinct functional classes. Thus, some functional specificity may be assigned by distinct histone methylation-mediated gene repression mechanisms, for example for genes regulating germlayer specification (Chan et al., 2009). A role of histone methylation as a mechanism of regulation of transcriptional repression is implied by the recent observation of uncoupling of DNA methylation and gene repression in *Xenopus* embryos (Bogdanovic et al., 2011). Functional specificity may also be determined by the combinatorial binding of transcription factors that regulate activity of *cis* regulatory elements during development (Zinzen et al., 2009). Of note, chromatin prepattering is likely to be important not only for early developmental decisions but also for cell fate determination during organogenesis (Xu et al., 2011).

An instructive role of histone marks for development is consistent with specific genes in pre-MBT stage embryos carrying the same marks in sperm (Wu et al., 2011). This is also in line with, in mammalian and zebrafish sperm, H3K4me3 or H3K27me3 marking of genes enriched in similar GO terms as pre-MBT H3K4me3-marked genes in our study (Hammoud et al., 2009; Brykczynska et al., 2010; Wu et al., 2011). Moreover, H3K27me3 decorates chromatin in mouse male pronuclei before ZGA (Albert and Peters, 2009; Puschendorf et al., 2008). These findings suggest that early developmental instructions may be provided by specific genomic positioning of histones marks in gametes, which may be transmitted to the embryo through fertilization (Puschendorf et al., 2008; Brykczynska et al., 2010; Arico et al., 2011). Proving this hypothesis will require additional data at stages that are technically challenging to examine due to the low level of modified histones (Vastenhouw et al., 2010) (this paper) and the sensitivity of current immunological approaches.

An alternative interpretation of our findings is a postfertilization reconstitution of epigenetic marks based on DNA sequence rather than through a copy of histone modifications on the replicated DNA in the embryo. Such a pattern would arguably not be inherited stricto sensu from gametes but represent an inherent instructive property of DNA. A reconstitution model on genes already bearing the marks in sperm would nonetheless argue that some instructive continuity be perpetuated. This may be at the level of histone variants (Wu et al., 2011), DNA methylation (Weber et al., 2007; Wu et al., 2011), transposons (Aravin et al., 2008), or small RNAs (Aravin and Bourc'his, 2008), all of which have been identified in sperm. Additional functional studies testing the significance of pre-MBT marking of the genome by histone modifications, and how prepatterning is determined will help elucidate processes taking place during pre-MBT stages as the embryo prepares for zygotic gene activation.

EXPERIMENTAL PROCEDURES

Antibodies

Antibodies used for ChIP-chip were to H3K4me3 (Diagenode 003-050), H3K27me3 (Millipore 07-449), H3K9me3 (Diagenode 056-050), H3K36me3 (Diagenode 058-050), and RNAPII (Santa Cruz sc-899). Antibodies used for ChIP-qPCR were to H3K4me3 (Diagenode or Millipore 07-473, as specified) and H3K27me3 (Millipore or Diagenode 069-050, as specified) and H3K9me3 (Diagenode). Antibodies used for carrier ChIP-PCR were anti-H3K4me3 (Abcam ab8580), anti-H3K9me3 (Millipore 07-442), and anti-H3K27me3 (Diagenode). Anti-H3K4me3 antibodies used for immunostaining were from Abcam (ab8580) and Cell Signaling (9727). Antibodies used for immunoblotting were from Diagenode (H3K4me3, H3K9me3, H3K36me3), Millipore (H3K27me3), Abcam (H3, ab1791), Santa Cruz (RNAPII, CTD4H8 sc47701), and Sigma-Aldrich (γ-tubulin, T5326).

Chromatin Immunoprecipitation

Zebrafish embryos at the pre-MBT, MBT, and post-MBT stages were respectively collected 2.5, 3.5, and 5.3 hpf, while monitoring developmental stage. Embryos were mechanically dechorionated, crosslinked and chromatin prepared as described (Lindeman et al., 2009). Chromatin was diluted to 0.25 U A_{260} for all embryo stages before ChIP, providing standardized amounts of input chromatin for each ChIP from each embryo stage. ChIP was performed (Lindeman et al., 2009) in three to six replicates with each antibody. For ChIP-chip, ChIP DNA was RNase-treated, amplified and amplification products were cleaned up, eluted, and processed for labeling and array hybridization (Roche-Nimblegen) or used for quantitative (q)PCR (Lindeman et al., 2010a).

Array Hybridization and Data Analysis

ChIP and input DNA was hybridized onto high-density promoter arrays described (Lindeman et al., 2010a). Signal intensity data were normalized using MA2C (Song et al., 2007). Each probe was assigned an MA2C score to reflect normalized and window-averaged $\log_2$ ChIP/Input ratios. For peak calling, a P-value cut-off of 10^{-4} was used. GO term enrichment was calculated using Bioconductor GOstats.

Carrier ChIP

Carrier ChIP was performed as described (O'Neill et al., 2006) with modifications. Embryos (n = 300) at the 256-cell stage were washed in ice-cold PBS/5 mM sodium butyrate. Cells were snap-frozen and stored at −20°C. Upon thawing, cells were mixed with *Drosophila* SL2 cells, suspended in 500 μl NB buffer (15 mM Tris-HCl [pH 7.4], 60 mM KCl, 15 mM NaCl, 5 mM $MgCl_2$, 0.1 mM EGTA, 0.5 mM 2-mercaptoethanol, 0.1 mM PMSF), mixed with 250 μl 1% Tween-40 in NB buffer and left on ice for 10 min. Nuclei were released by 5 strokes in a Dounce homogenizer, sedimented (100 g, 15 min, 4°C), washed in 1 ml NB/5% sucrose and resedimented (100 g, 20 min. 4°C). Nuclei were resuspended in digestion buffer (50 mM Tris-HCl [pH 7.4], 0.32 M sucrose, 4 mM $MgCl_2$, 1 mM $CaCl_2$, 0.1 mM PMSF) to 0.5 mg/ml chromatin. Chromatin was digested with 50 U micrococcal nuclease for 5 min at 28°C, sedimented (100 g, 20 min, 4°C) and the supernatant (S1) was transferred to a new tube. The pellet was resuspended in 400 μl lysis buffer (2 mM Tris-HCl [pH 7.4], 0.2 mM EDTA, 5 mM sodium butyrate, 0.2 mM PMSF) and dialyzed overnight against lysis buffer and the dialyzed fraction centrifuged (100 g, 10 min). The supernatant was pooled with S1 and used for ChIP using antibodies to H3K4me3 (Abcam), H3K9me3 (Diagenode) and H3K27me3 (Diagenode).

Polymerase Chain Reaction

Quantitative (q)PCR and RT-PCR conditions and primers are described in Supplemental Experimental Procedures.

RNA Sequencing and Developmental Gene Clustering

RNA-seq data (available in GEO under accession number GSE22830) were from a parallel study investigating the transcriptome of early zebrafish embryos (Aanes et al., 2011). For consistency with promoter array data, reads were mapped to Zv7 using Bioscope v1.1 (Applied Biosystems) and mapped reads were counted for each RefSeq annotation. Read counts were first normalized to account for global shifts in RNA expression during development, then normalized to transcript length. Expression data were mapped to NCBI Gene IDs covered by the Nimblegen array to allow gene-level correlation between expression and histone modifications. The clustering strategy used to generate cohorts of genes defined as maternal, maternal-zygotic and with nondetected transcripts is described in Supplemental Experimental Procedures.

Immunofluorescence

Embryos were fixed in 4% PFA, 125 mM HEPES (pH 7.6; 30 min, 4°C), re-fixed in 8% PFA, 125 mM HEPES (pH 7.6; 60 min, 4°C) followed by permeabilization in 0.5% Triton X-100 in PBS (30 min, gentle rocking). Embryos were blocked in 10% NBCS (Sigma-Aldrich) for 1 hr and immunolabeled with primary antibody overnight at 4°C. Embryos were washed in PBS and incubated in anti-rabbit-HRP (1:200) overnight at 4°C. Embryos were washed in PBS and incubated in Cyanine 3 Tyramide diluted 1:50 in Amplification Reagent (NEL704A, PerkinElmer) for 30 min. Embryos were washed in PBS and mounted in VectaShield containing DAPI (Vector Labs). Images were taken with a Zeiss LSM-S10 confocal microscope.

Western Blotting

Embryos at each developmental stage examined were dechorionated using Pronase (1 mg/ml; Sigma-Aldrich) for 5-10 min at room temperature. After washing in PBS, embryos were transferred to 500 μl of deyolking solution (55 mM NaCl, 1.8 mM KCl, 1.25 mM $NaHCO_3$) and sedimented for 30 s at 4°C. After washing in PBS, cell pellets were snap-frozen and stored at −80°C until use. After thawing, cells were lysed in 1 × SDS sample buffer containing protease inhibitors (eComplete, Roche), immediately heated at 70°C for 5 min and kept on ice until loading on a 4%–20% Tris-HCl gel. For analysis of H3K4me3, H3K9me3, H3K27me3, H3K36me3, and γ-tubulin, numbers of embryo equivalents loaded per lane were 150, 100, and 25 for pre-MBT, MBT and post-MBT stages respectively. For H3 and RNAPII, 20 embryo equivalents were loaded for each developmental stage. Immunoblotting and visualization were according to the Odyssey System (LI-COR Biosciences). Antibody dilutions were 1:1000 for H3K4me3, H3K27me3, H3K36me3 and H3, 1:500 for H3K9me3 and RNAPII CTD4H8, and 1:10,000 for γ-tubulin.

ACCESSION NUMBERS

ChIP-chip data have been deposited in NCBI GEO with accession code number GSE27314.

SUPPLEMENTAL INFORMATION

Supplemental Information includes four figures, five tables, and Supplemental Experimental Procedures and can be found with this article online at doi:10.1016/j.devcel.2011.10.008.

ACKNOWLEDGMENTS

We thank Lars Moen and the Norwegian Zebrafish Platform for technical assistance and Dr. Laura O'Neill (University of Birmingham) for advice on carrier ChIP. This work was supported by A*STAR (Singapore; to C.W. and S.M.), the *Dopaminet* project of the FP7 EU program (to F.M.), the Research Council of Norway (to P.A. and P.C.) and the Norwegian Stem Cell Center (to P.C.).

Received: April 13, 2011
Revised: August 12, 2011
Accepted: October 11, 2011
Published online: December 1, 2011

REFERENCES

Aanes, H., Winata, C.L., Lin, C.H., Chen, J.P., Srinivasan, K.G., Lee, S.G., Lim, A.Y., Hajan, H.S., Collas, P., Bourque, G., et al. (2011). Zebrafish mRNA sequencing deciphers novelties in transcriptome dynamics during maternal to zygotic transition. Genome Res. *21*, 1328–1338.

Aday, A.W., Zhu, L.J., Lakshmanan, A., Wang, J., and Lawson, N.D. (2011). Identification of cis regulatory features in the embryonic zebrafish genome through large-scale profiling of H3K4me1 and H3K4me3 binding sites. Dev. Biol. *357*, 450–462.

Akkers, R.C., van Heeringen, S.J., Jacobi, U.G., Janssen-Megens, E.M., Françoijs, K.J., Stunnenberg, H.G., and Veenstra, G.J. (2009). A hierarchy of H3K4me3 and H3K27me3 acquisition in spatial gene regulation in Xenopus embryos. Dev. Cell *17*, 425–434.

Albert, M., and Peters, A.H. (2009). Genetic and epigenetic control of early mouse development. Curr. Opin. Genet. Dev. *19*, 113–121.

Aravin, A.A., and Bourc'his, D. (2008). Small RNA guides for de novo DNA methylation in mammalian germ cells. Genes Dev. *22*, 970–975.

Aravin, A.A., Sachidanandam, R., Bourc'his, D., Schaefer, C., Pezic, D., Toth, K.F., Bestor, T., and Hannon, G.J. (2008). A piRNA pathway primed by individual transposons is linked to de novo DNA methylation in mice. Mol. Cell *31*, 785–799.

Arico, J.K., Katz, D.J., van der Vlag, J., and Kelly, W.G. (2011). Epigenetic patterns maintained in early Caenorhabditis elegans embryos can be established by gene activity in the parental germ cells. PLoS Genet. *7*, e1001391.

Azuara, V., Perry, P., Sauer, S., Spivakov, M., Jørgensen, H.F., John, R.M., Gouti, M., Casanova, M., Warnes, G., Merkenschlager, M., and Fisher, A.G. (2006). Chromatin signatures of pluripotent cell lines. Nat. Cell Biol. *8*, 532–538.

Barski, A., Cuddapah, S., Cui, K., Roh, T.Y., Schones, D.E., Wang, Z., Wei, G., Chepelev, I., and Zhao, K. (2007). High-resolution profiling of histone methylations in the human genome. Cell *129*, 823–837.

Bernstein, B.E., Mikkelsen, T.S., Xie, X., Kamal, M., Huebert, D.J., Cuff, J., Fry, B., Meissner, A., Wernig, M., Plath, K., et al. (2006). A bivalent chromatin structure marks key developmental genes in embryonic stem cells. Cell *125*, 315–326.

Bilodeau, S., Kagey, M.H., Frampton, G.M., Rahl, P.B., and Young, R.A. (2009). SetDB1 contributes to repression of genes encoding developmental regulators and maintenance of ES cell state. Genes Dev. *23*, 2484–2489.

Blythe, S.A., Cha, S.W., Tadjuidje, E., Heasman, J., and Klein, P.S. (2010). beta-Catenin primes organizer gene expression by recruiting a histone H3 arginine 8 methyltransferase, Prmt2. Dev. Cell *19*, 220–231.

Bogdanovic, O., Long, S.W., van Heeringen, S.J., Brinkman, A.B., Gómez-Skarmeta, J.L., Stunnenberg, H.G., Jones, P.L., and Veenstra, G.J. (2011). Temporal uncoupling of the DNA methylome and transcriptional repression during embryogenesis. Genome Res. *21*, 1313–1327.

Brykczynska, U., Hisano, M., Erkek, S., Ramos, L., Oakeley, E.J., Roloff, T.C., Beisel, C., Schübeler, D., Stadler, M.B., and Peters, A.H. (2010). Repressive and active histone methylation mark distinct promoters in human and mouse spermatozoa. Nat. Struct. Mol. Biol. *17*, 679–687.

Carrozza, M.J., Li, B., Florens, L., Suganuma, T., Swanson, S.K., Lee, K.K., Shia, W.J., Anderson, S., Yates, J., Washburn, M.P., and Workman, J.L. (2005). Histone H3 methylation by Set2 directs deacetylation of coding regions by Rpd3S to suppress spurious intragenic transcription. Cell *123*, 581–592.

Chan, T.M., Longabaugh, W., Bolouri, H., Chen, H.L., Tseng, W.F., Chao, C.H., Jang, T.H., Lin, Y.I., Hung, S.C., Wang, H.D., and Yuh, C.H. (2009). Developmental gene regulatory networks in the zebrafish embryo. Biochim. Biophys. Acta *1789*, 279–298.

Cui, K., Zang, C., Roh, T.Y., Schones, D.E., Childs, R.W., Peng, W., and Zhao, K. (2009). Chromatin signatures in multipotent human hematopoietic stem

cells indicate the fate of bivalent genes during differentiation. Cell Stem Cell *4*, 80–93.

Dahl, J.A., Reiner, A.H., Klungland, A., Wakayama, T., and Collas, P. (2010). Histone H3 lysine 27 methylation asymmetry on developmentally-regulated promoters distinguish the first two lineages in mouse preimplantation embryos. PLoS ONE *5*, e9150.

Dey, A., Chitsaz, F., Abbasi, A., Misteli, T., and Ozato, K. (2003). The double bromodomain protein Brd4 binds to acetylated chromatin during interphase and mitosis. Proc. Natl. Acad. Sci. USA *100*, 8758–8763.

Ernst, J., Kheradpour, P., Mikkelsen, T.S., Shoresh, N., Ward, L.D., Epstein, C.B., Zhang, X., Wang, L., Issner, R., Coyne, M., et al. (2011). Mapping and analysis of chromatin state dynamics in nine human cell types. Nature *473*, 43–49.

Graveley, B.R., Brooks, A.N., Carlson, J.W., Duff, M.O., Landolin, J.M., Yang, L., Artieri, C.G., van Baren, M.J., Boley, N., Booth, B.W., et al. (2011). The developmental transcriptome of Drosophila melanogaster. Nature *471*, 473–479.

Hammoud, S.S., Nix, D.A., Zhang, H., Purwar, J., Carrell, D.T., and Cairns, B.R. (2009). Distinctive chromatin in human sperm packages genes for embryo development. Nature *460*, 473–478.

Hawkins, R.D., Hon, G.C., Lee, L.K., Ngo, Q., Lister, R., Pelizzola, M., Edsall, L.E., Kuan, S., Luu, Y., Klugman, S., et al. (2010). Distinct epigenomic landscapes of pluripotent and lineage-committed human cells. Cell Stem Cell *6*, 479–491.

Jeong, Y.S., Yeo, S., Park, J.S., Lee, K.K., and Kang, Y.K. (2007). Gradual development of a genome-wide H3-K9 trimethylation pattern in paternally derived pig pronucleus. Dev. Dyn. *236*, 1509–1516.

Kane, D.A., and Kimmel, C.B. (1993). The zebrafish midblastula transition. Development *119*, 447–456.

Kharchenko, P.V., Alekseyenko, A.A., Schwartz, Y.B., Minoda, A., Riddle, N.C., Ernst, J., Sabo, P.J., Larschan, E., Gorchakov, A.A., Gu, T., et al. (2011). Comprehensive analysis of the chromatin landscape in Drosophila melanogaster. Nature *471*, 480–485.

Kolasinska-Zwierz, P., Down, T., Latorre, I., Liu, T., Liu, X.S., and Ahringer, J. (2009). Differential chromatin marking of introns and expressed exons by H3K36me3. Nat. Genet. *41*, 376–381.

Leung, T., Söll, I., Arnold, S.J., Kemler, R., and Driever, W. (2003). Direct binding of Lef1 to sites in the boz promoter may mediate pre-midblastula-transition activation of boz expression. Dev. Dyn. *228*, 424–432.

Lindeman, L.C., Vogt-Kielland, L.T., Aleström, P., and Collas, P. (2009). Fish'n ChIPs: chromatin immunoprecipitation in the zebrafish embryo. Methods Mol. Biol. *567*, 75–86.

Lindeman, L.C., Reiner, A.H., Mathavan, S., Aleström, P., and Collas, P. (2010a). Tiling histone H3 lysine 4 and 27 methylation in zebrafish using high-density microarrays. PLoS ONE *5*, e15651.

Lindeman, L.C., Winata, C.L., Aanes, H., Mathavan, S., Alestrom, P., and Collas, P. (2010b). Chromatin states of developmentally-regulated genes revealed by DNA and histone methylation patterns in zebrafish embryos. Int. J. Dev. Biol. *54*, 803–813.

Mathavan, S., Lee, S.G., Mak, A., Miller, L.D., Murthy, K.R., Govindarajan, K.R., Tong, Y., Wu, Y.L., Lam, S.H., Yang, H., et al. (2005). Transcriptome analysis of zebrafish embryogenesis using microarrays. PLoS Genet. *1*, 260–276.

Müller, F., Lakatos, L., Dantonel, J., Strähle, U., and Tora, L. (2001). TBP is not universally required for zygotic RNA polymerase II transcription in zebrafish. Curr. Biol. *11*, 282–287.

O'Neill, L.P., VerMilyea, M.D., and Turner, B.M. (2006). Epigenetic characterization of the early embryo with a chromatin immunoprecipitation protocol applicable to small cell populations. Nat. Genet. *38*, 835–841.

Pan, G., Tian, S., Nie, J., Yang, C., Ruotti, V., Wei, H., Jonsdottir, G.A., Stewart, R., and Thomson, J.A. (2007). Whole-genome analysis of histone H3 lysine 4 and lysine 27 methylation in human embryonic stem cells. Cell Stem Cell *1*, 299–312.

Puschendorf, M., Terranova, R., Boutsma, E., Mao, X., Isono, K., Brykczynska, U., Kolb, C., Otte, A.P., Koseki, H., Orkin, S.H., et al. (2008). PRC1 and Suv39h specify parental asymmetry at constitutive heterochromatin in early mouse embryos. Nat. Genet. *40*, 411–420.

Ruthenburg, A.J., Li, H., Patel, D.J., and Allis, C.D. (2007). Multivalent engagement of chromatin modifications by linked binding modules. Nat. Rev. Mol. Cell Biol. *8*, 983–994.

Schier, A.F. (2007). The maternal-zygotic transition: death and birth of RNAs. Science *316*, 406–407.

Schuettengruber, B., Ganapathi, M., Leblanc, B., Portoso, M., Jaschek, R., Tolhuis, B., van Lohuizen, M., Tanay, A., and Cavalli, G. (2009). Functional anatomy of polycomb and trithorax chromatin landscapes in Drosophila embryos. PLoS Biol. *7*, e13.

Shechter, D., Nicklay, J.J., Chitta, R.K., Shabanowitz, J., Hunt, D.F., and Allis, C.D. (2009). Analysis of histones in Xenopus laevis. I. A distinct index of enriched variants and modifications exists in each cell type and is remodeled during developmental transitions. J. Biol. Chem. *284*, 1064–1074.

Song, J.S., Johnson, W.E., Zhu, X., Zhang, X., Li, W., Manrai, A.K., Liu, J.S., Chen, R., and Liu, X.S. (2007). Model-based analysis of two-color arrays (MA2C). Genome Biol. *8*, R178.

Sun, X.J., Xu, P.F., Zhou, T., Hu, M., Fu, C.T., Zhang, Y., Jin, Y., Chen, Y., Chen, S.J., Huang, Q.H., et al. (2008). Genome-wide survey and developmental expression mapping of zebrafish SET domain-containing genes. PLoS ONE *3*, e1499.

Tadros, W., and Lipshitz, H.D. (2009). The maternal-to-zygotic transition: a play in two acts. Development *136*, 3033–3042.

Terrenoire, E., McRonald, F., Halsall, J.A., Page, P., Illingworth, R.S., Taylor, A.M., Davison, V., O'Neill, L.P., and Turner, B.M. (2010). Immunostaining of modified histones defines high-level features of the human metaphase epigenome. Genome Biol. *11*, R110.

Thomson, J.P., Skene, P.J., Selfridge, J., Clouaire, T., Guy, J., Webb, S., Kerr, A.R., Deaton, A., Andrews, R., James, K.D., et al. (2010). CpG islands influence chromatin structure via the CpG-binding protein Cfp1. Nature *464*, 1082–1086.

Toyama, R., Rebbert, M.L., Dey, A., Ozato, K., and Dawid, I.B. (2008). Brd4 associates with mitotic chromosomes throughout early zebrafish embryogenesis. Dev. Dyn. *237*, 1636–1644.

Vastenhouw, N.L., Zhang, Y., Woods, I.G., Imam, F., Regev, A., Liu, X.S., Rinn, J., and Schier, A.F. (2010). Chromatin signature of embryonic pluripotency is established during genome activation. Nature *464*, 922–926.

Wang, Z., Zang, C., Rosenfeld, J.A., Schones, D.E., Barski, A., Cuddapah, S., Cui, K., Roh, T.Y., Peng, W., Zhang, M.Q., and Zhao, K. (2008). Combinatorial patterns of histone acetylations and methylations in the human genome. Nat. Genet. *40*, 897–903.

Weber, M., Hellmann, I., Stadler, M.B., Ramos, L., Pääbo, S., Rebhan, M., and Schübeler, D. (2007). Distribution, silencing potential and evolutionary impact of promoter DNA methylation in the human genome. Nat. Genet. *39*, 457–466.

Wu, S.F., Zhang, H., and Cairns, B.R. (2011). Genes for embryo development are packaged in blocks of multivalent chromatin in zebrafish sperm. Genome Res. *21*, 578–589.

Xu, C.R., Cole, P.A., Meyers, D.J., Kormish, J., Dent, S., and Zaret, K.S. (2011). Chromatin "prepattern" and histone modifiers in a fate choice for liver and pancreas. Science *332*, 963–966.

Zinzen, R.P., Girardot, C., Gagneur, J., Braun, M., and Furlong, E.E. (2009). Combinatorial binding predicts spatio-temporal cis-regulatory activity. Nature *462*, 65–70.